

GLOBAL JOURNAL OF ENGINEERING SCIENCE AND RESEARCHES ATMOSPHERIC CORRECTION OF VISIBLE CHANNEL OF SATELLITE IMAGE FROM INSAT-3D IMAGER USING SECOND SIMULATION OF THE SATELLITE SIGNAL IN THE SOLAR SPECTRUM - 6S MODEL

M.Sakthivel^{*1}, Manoj Hari² & Dharani G³

^{*1}Associate Professor, University of Madras, India

²M.Sc Student, University of Madras, India

³M.Sc Student, University of Madras, India

ABSTRACT

Atmospheric correction is an important pre-processing step required in many satellite remote sensing applications. Although there are several available atmospheric correction algorithms, there is limited literature available that examines their effectiveness using in situ measurements from spectroradiometers to retrieve reflectance. The aim of this study is to atmospherically correct the satellite image using Second Simulation of a Satellite Signal in the Solar Spectrum-6S Radiative Transfer Model and to conduct an accuracy assessment of the results using in-situ measurements from spectroradiometers. Look-up table (LUT) for surface reflectance was generated under different conditions of solar zenith/azimuth angles and satellite zenith/azimuth angles based on the Second Simulation of the Satellite Signal in the Solar Spectrum radiative transfer model, wherein correction for aerosols, water vapour and ozone was also done. Zenith angles were taken at 5⁰ interval and azimuth angles were taken at 10⁰ intervals for calculation of surface reflectance in LUT. All these simulations were done for visible channel (0.55µm to 0.75µm) and considering tropical atmosphere and Lambertian surface. The LUT developed was used for atmospheric correction of visible images of INSAT-3D imager to get an estimate surface reflectance values.

Key Words: Atmospheric Correction, 6S, INSAT-3D Imager, LUT.

I. INTRODUCTION

Atmospheric correction is an important pre-processing step required in many satellite remote sensing applications (Hadjimitsis, 2009). Although there are several available atmospheric correction methods, there is limited literature available that utilizes atmospheric correction methods to retrieve aerosol optical thickness (AOT) (Hadjimitsis et al., 2010)

II. METHODOLOGY

Research indicates that, among all other atmospheric correction methods, the Second Simulation of the Satellite Signal in the Solar Spectrum, 6S Model focused on in this study is considered to be one of the most effective methods for atmospheric correction (Liang et al., 2001).

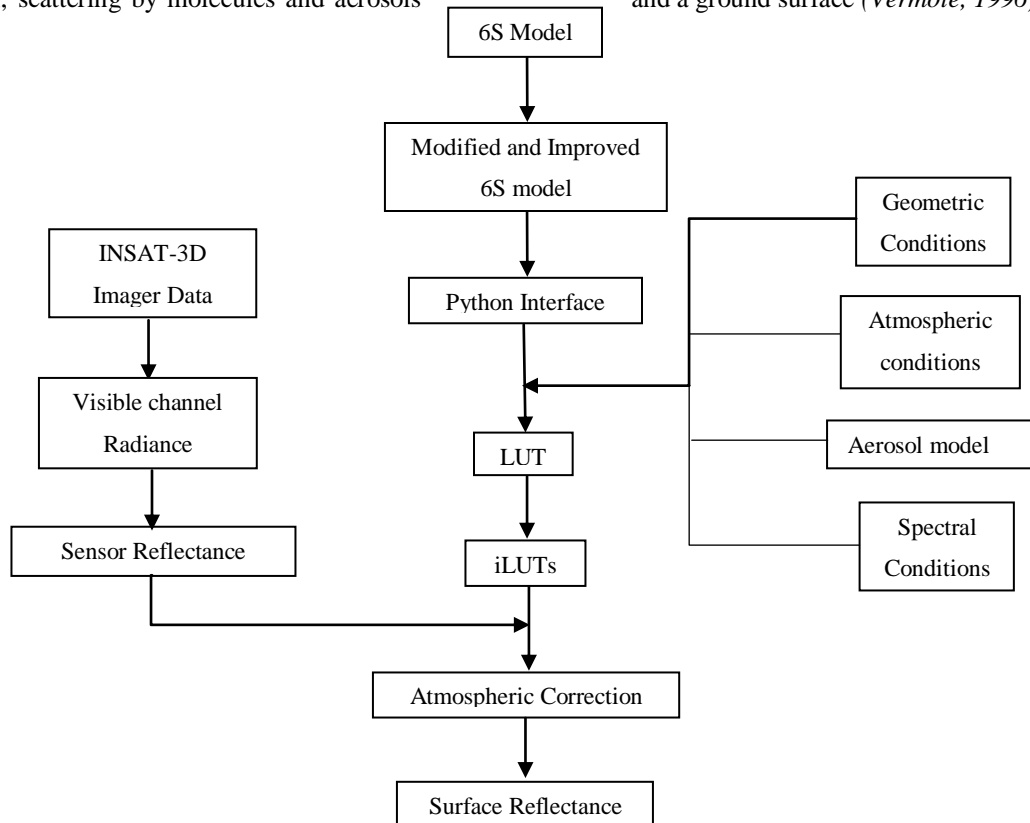
The overall methodology that has been used in this study is based on the following components:

- First, to improve the existing Second Simulation of the Satellite Signal in the Solar Spectrum atmospheric correction method by developing the codes with effectiveness
- Second, using the python interface of Second Simulation of the Satellite Signal in the Solar Spectrum atmospheric correction methods to create Look-up Table to perform the surface reflectance.
- Finally, using the sensor radiance the surface reflectance is calculated by correlating it with the developed Look-up table and apply the fast atmospheric correction using surface reflectance.

A computer code in python interface predicts a satellite signal of atmosphere without clouds between 0.25 and 4.0 μm. At the satellite level for Lambertian surface, the apparent reflectance is written as,

$$\rho'(\theta_s, \theta_v, \phi_v) = t_g(\theta_s, \theta_v) \left\{ \rho_a(\theta_s, \theta_v, \phi_v) + \frac{T(\theta_s)}{1 - \langle \rho(M) \rangle} \left[\rho_c(M) e^{-\frac{\tau}{\mu_v}} + \langle \rho(M) \rangle t_d(\theta_v) \right] \right\}$$

For the main atmospheric effects the above formalism was taken into account, gaseous absorption by H₂O, O₂, CO₂ and O₃, scattering by molecules and aerosols and a ground surface (Vermeete, 1996).



The following input parameters are necessary:

- Geometrical conditions,
- Atmospheric model for gaseous components,
- Aerosol model (type and concentration),
- Spectral condition,
- Ground reflectance (type and spectral variation).

At each step, it can be selected a proposed standard conditions or it can be defined as per the conditions that required. It is to be noted that the satellite navigation is done by a rough calculation from the nominal characteristics of the satellite orbit. It is obvious that, without anchor points, the localization is not very accurate (Vermeete, 1996).

At any wavelength, it can be interpolated from these values by assuming the spectral dependence

$$f(\lambda) = f(\lambda_0) \left(\frac{\lambda}{\lambda_0} \right)^{-\alpha}$$

and compute the apparent reflectance from the first equation.

Study Area

The satellite data that acquired from INSAT-3D Imager covers the Indian peninsula and its surrounding area in the Southeast Asia includes all the major countries and the Indian Ocean with the domain extension of 40°S-40°N and

30°E-120°E. Interested area that has been used to analyse the process of atmospheric correction is Chennai where it is located in the Tropical belt because the area includes wet and dry climate (*Köppen: Aw*)

Parameter determination in Lookup Table

Using look-up table to determine radiation properties of ground targets can improve the efficiency of the simulation image output. 6S model needs lots of parameters, and the output information is complex, in order to establish the look-up table both have data completeness and numerical computation efficiency, we need to complete two preparations (*Vermote, 1996*). The first one is to streamline the input parameters, its purpose is according to the sensitivity of input parameters to atmospheric radiative transfer information calculation precision, to select the most representative input parameters as the variables in look-up table, improve the look-up table generating efficiency; the second one is to make changes to 6S source code, make its output information only contains the brightness values of the ground targets related to independent variable at the sensor into the pupil, simplify the process of finding data in look-up table generating, and to further improve the look-up table generating efficiency (*Zhang, 1996; Jiang et al., 2011*).

III. AN OVERVIEW OF THE 6S ALGORITHM

The 6S algorithm is widely used and has been extensively tested to ensure accuracy (*Kotchenova et al., 2006*); it has gone through several evolutions and in its current state it is known as “6SV1.1.” This version has several important modifications when compared to some older versions, including the addition of polarization effects, something that has a substantial effect on the accuracy of the method (*Kotchenova and Vermote, 2007*). When operating in atmospheric correction mode, 6S allows the user to enter a Top of Atmosphere (ToA) reflectance, $\rho_{ToA}(\theta_s, \theta_v, \phi_r)$, at given solar zenith, view zenith, and relative azimuth angles. In general, these angular conditions are computed within the 6S code based on user selected conditions such as sensor type, pixel location, and time of year.

6S will then compute the land surface reflectance, ρ_s , by using the following equation:

$$\rho_s(\theta_s, \theta_v, \phi_r) = \frac{\rho_s}{1+S\rho_s}$$

with

$$\rho'_s = \left\{ \frac{[\rho_{ToA}(\theta_s, \theta_v, \phi_r)/T_G] - [\rho_a(\theta_s, \theta_v, \phi_r)]}{T_{\theta_s} T_{\theta_v}} \right\}$$

Atmospheric reflectance was calculated by the successive order of scattering (SOS) method that allows multiple scattering events to be considered and divides the atmosphere into a series of layers, each of which is individually examined (*Lenoble et al., 2007*). The idea behind this method is that it considers separate cases for where photons have been scattered once, twice, ..., N times. The results of each case are then summed to realize the total scattering contribution and the method is described in detail by (*Min and Duan, 2004*):

$$I(\tau, \mu_s, \mu_v, \phi) = \sum_{n=1}^N I^n(\tau, \mu_s, \mu_v, \phi)$$

Initially only primary scattering is considered, which in the case of upward radiation is calculated by equation

$$I^1(\tau; \mu_v, \phi) = \frac{\omega_0}{4\pi} \pi F_0 P(\mu_v, \phi_v; \mu_s, \phi_s) \exp\left(\frac{-\tau}{\mu_s}\right)$$

Once the primary scattering contribution is determined the higher orders of scattering, n , can be computed by

$$I^n(\tau; \mu_v, \phi) = \frac{1}{\mu} \sum_{j=i}^p J^n(\tau_j; -\mu_v, \phi) \exp\left[\frac{(\tau_j - \tau)}{-\mu}\right] \Delta\tau$$

where p specifies the number of layers used to represent the atmosphere, τ_j is the optical thickness within layer j , and $\Delta\tau$ is the difference in optical depth between layer $j = x$ and $j = x + 1$. J^n is computed based on the radiation emitted from I^{n-1} as follows:

$$J^n(\tau_j; -\mu_v, \phi) = \frac{\omega_0}{4\pi} \int_0^{2\pi} \int_{-1}^1 I^{n-1}(\tau; \mu', \phi') P(\mu_v, \phi_v; \mu', \phi') \cdot d\mu' \cdot d\phi'$$

The number of scattering orders required varies dependent on the optical conditions encountered, although under the majority of conditions convergence of the solution to within acceptable limits occurs within 5–10 orders of scattering (Min and Duan, 2004).

The final components within the atmospheric correction scheme are the incoming and outgoing atmospheric transmittances, which can be calculated from the total illumination at the Earth’s surface:

$$E^{total}(\theta_s) = \frac{T(\theta_s)}{1 - \rho_s S}$$

where the total downward transmittance, $T(\theta_s)$, can be calculated from:

$$T(\theta_s) = \exp\left(\frac{-\tau}{\mu_s}\right) + t_d(\theta_s)$$

Literature studies comparing 6S to other complex atmospheric correction schemes such as MODTRAN or a Monte Carlo simulation have shown that the 6S method is highly accurate under a wide range of conditions, including those expected to be seen within a typical MSG-SEVIRI scene (Kotchenova et al., 2008).

Python interface of 6S – Py6S

Py6S is a Python interface to the 6S model which has been developed to address the limitations described above. By not re-implementing the model itself, we can ensure that results produced using

- User-friendly parameter setting, with easily-accessible documentation
- Helper functions making common operations simple
- Plotting capabilities
- Access to all other Python functionality
- Ability to import parameters from external data sources
- Reproducibility

IV. LOOK-UP TABLE

The methodology flow chart gives an overview of surface reflectance retrievals and their validation. A LUT is produced using 6S and the input parameters as described.

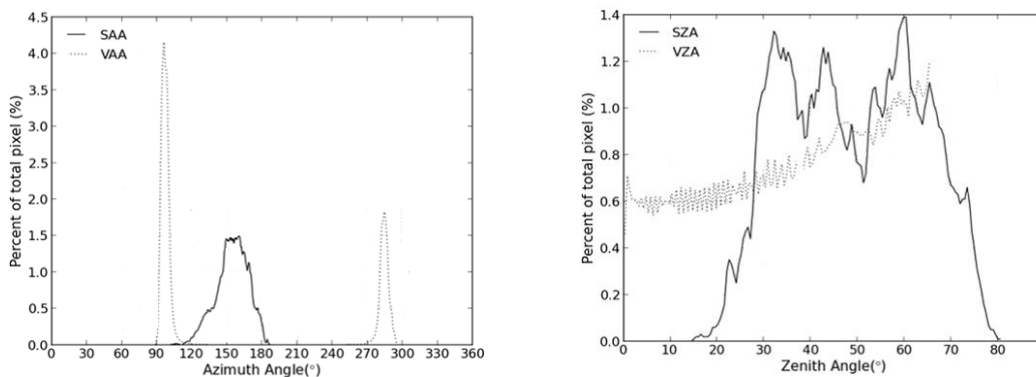


Figure. 1. Diagram of the angular distribution azimuth angle and zenith angle respectively in which the different lines denote geometry (solid: solar azimuth and zenith, dotted: viewing azimuth and zenith)

The produced LUT has a seven-dimensional structure corresponding to seven input parameters (SZA, VZA, SAA, VAA, AOD, water vapour, and ozone). The LUT was generated with the angles that can be covered by INSAT. Both solar and viewing zenith angles range from 0 to 80°, whereas azimuth angles range from 0 to 360°.

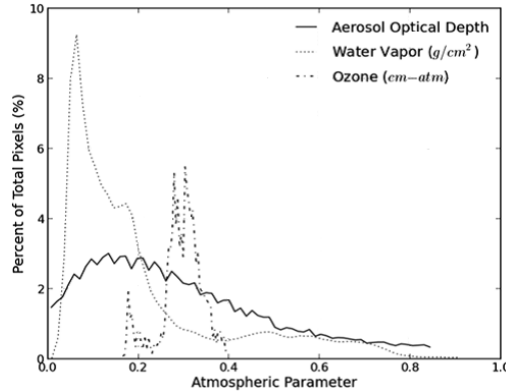


Figure. 2. Histogram of atmospheric parameters (solid: AOD, dotted: Water Vapour, dash-dot: Ozone)

A continental aerosol model (Vermote et al., 2006) was used to create the LUT using the 6S. Water vapor and ozone column densities obtained from AERONET (AEROSOL ROBOTICS NETWORK) were used as trace gas inputs. The surface state was assumed to have a homogeneous Lambertian vegetative reflectance and no directional effect (Lyapustin et al., 2011). Three correction coefficients called xa, xb, and xc; they were produced directly from 6S calculations. xa denotes the path radiance in reflectance unit, xb is the total diffuse transmittance of the atmosphere accordance with solar beam incoming and satellite view direction, and xc represents the reflectance of the atmosphere for isotropic light entering the base of the atmosphere (Vermote and Vermeulen, 1999). With pre-computed coefficients, the following were used to retrieve the surface reflectance information

$$y = (xa \times L) - xb$$

$$acr = \frac{y}{1 + (xc \times y)}$$

In the above equations, L (in $Wm^{-2}sr^{-1} \mu m^{-1}$) is the top of atmosphere (TOA) radiance measured by the satellite sensor, and acr is the final corrected surface reflectance (Zhao et al. (2000) to correct atmospheric effect for estimating albedo.

Table. 1. Range and interval of input parameters for the LUT coarse and fine (angular and atmospheric parameters).

Parameters (Units)	Coarse Interval			Fine Interval		
	Minimu m	Maxim um	Interv al	Minimu m	Maxim um	Interv al
Solar Zenith Angle-SZA (degree)	0	80	10	0	75	5
Solar Azimuth Angle-SAA (degree)	0	360	10	0	180	10
View Zenith Angle-VZA (degree)	0	80	10	0	75	5
View Azimuth Angle-SZA (degree)	0	360	10	0	180	10
Water Vapour Content (gm cm ⁻²)	0	5	0.5	0	8	0.5
Ozone content (cm-atm)	0	1	0.2	0	1	0.2
Aerosol Optical Depth (τ550)	0	1	0.25	0	1	0.1

V. PERFORMANCE OF THE NEW 6S-BASED LUT

In this study a standard atmospheric model proposed by 6S code (the Tropical atmospheric model) was used. There are two reasons why the standard atmosphere model was chosen for this study. First, measurement of atmospheric characteristics on the day of satellite overpass and input into radiative transfer code (6S) for the purpose of atmospheric correction is accurate but too expensive and time-consuming to be used on an operational basis (Teillet, 1992). Therefore, it is likely to be chosen the standard atmosphere model that was provided by the atmospheric code 6S to illustrate the feasibility of the simple atmospheric correction method. Second, Moran et al. (1992) and Lei et al. (1998) report that the effect on accuracy of atmospheric correction obtained from a standard atmosphere model is comparable to that obtained from an in-site model (errors are ± 0.02 and 0.02 for surface reflectance and irradiance, respectively). These results give the confidence in the choice of the standard atmosphere model (Teillet, 1992). For this study we also used a standard aerosol model (the continental aerosol model) to define aerosol type. To define the concentration of aerosols, a meteorological parameter (the value of the horizontal visibility in km) should be entered directly into 6S.

To account for spectral condition and ground reflectance, all six reflective TM bands are used, and homogeneous Lambertian vegetative reflectance characteristics are assumed. The surface is considered as Lambertian here, because most satellite-borne instruments only measure radiance reflected in one direction. A BRDF model (Walthall et al's., 1985) was employed to retrieve albedo from atmospherically corrected reflectance for natural surface (anisotropic surface).

Performance of the generated LUT

When processing satellite data collected over a large area such as on the national scale, fast run time is essential. SMAC is a simple and fast atmospheric correction model that is about 1000 times faster than 6S (Rahman and Dedieu, 1994) when performing surface reflectance retrieval. But the accuracy level is highly reliable over the results produced using 6S. The time required for the correction methods using personal computer with Intel i5 Quad Core CPU and 16GB memory. The total measured run time, which is the sum of the time spent for all pixels within the study area, was averaged. For accurate comparison, each run-time (LUT (fine interval): $1.571e-5$ second/pixel, LUT (coarse interval): $1.558e-5$ second/pixel) does not include the time taken for the collocation of input parameters. Overall, these results indicate that our new LUT has a high potential for operational purposes in terms of both accuracy and run time.

This study demonstrates that the produced new SZA interval of LUT can be a useful for the retrieval of surface reflectance from satellite observation data in the visible channel. Result of analyses showed suggested interval of SZA is suitable for over 70° zenith angle range.

VI. RESULTS

This study demonstrates that the new SZA interval of LUT can be a useful for the retrieval of surface reflectance from satellite observation data in the visible band. Result of analyses showed suggested interval of SZA is suitable for over 60° zenith angle range. LUT is effective way to overcome long and complex calculation of RTM for atmospheric correction.

The result produced the first 6S-based LUT for the retrieval of surface reflectance, which covers not only low but also high SZAs with high accuracy and short run-times in the visible band. The surface reflectance obtained from this LUT was also generally in good agreement with INSAT - 3D Imager data.

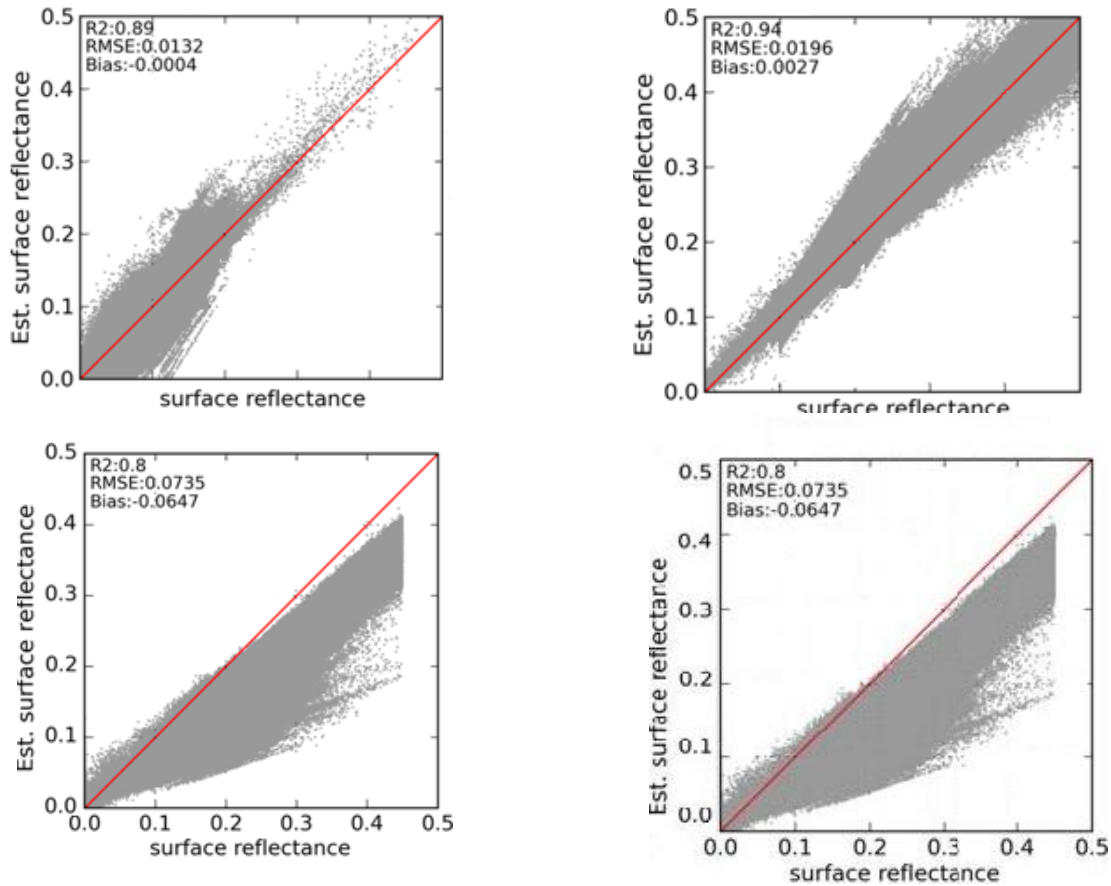
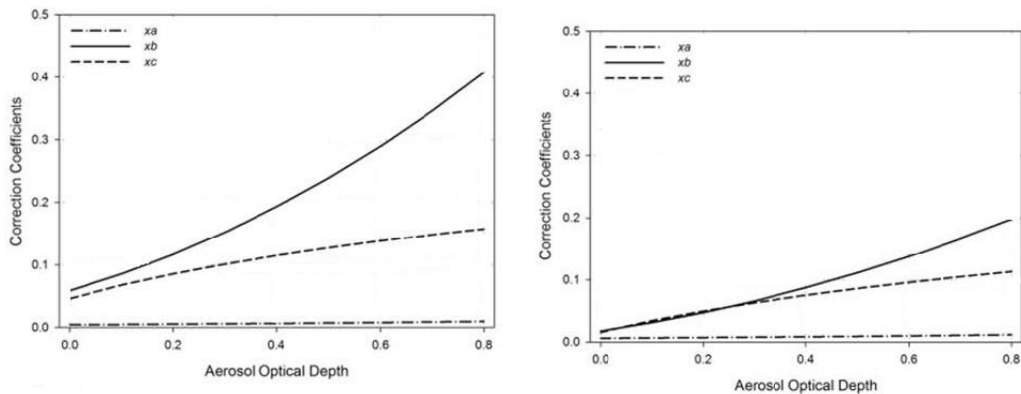


Figure 3. Scatter plot of coarse interval reflectance against estimated fine interval reflectance for various solar zenith angle (Clockwise from top left: 40-50, 50-60, 60-70, and 70-80)

However, uncertainties remained at high SZAs, which reduced the accuracy of the retrieved surface reflectance. To improve the accuracy of the retrieved surface reflectance at high SZAs, we produced an LUT with a finer SZA interval 5° at high SZAs. Thus, it is attempted to identify the contribution of each input parameter of the LUT to these correlations by conducting a sensitivity analysis of the correction coefficients and input parameters, as shown in the following figures.



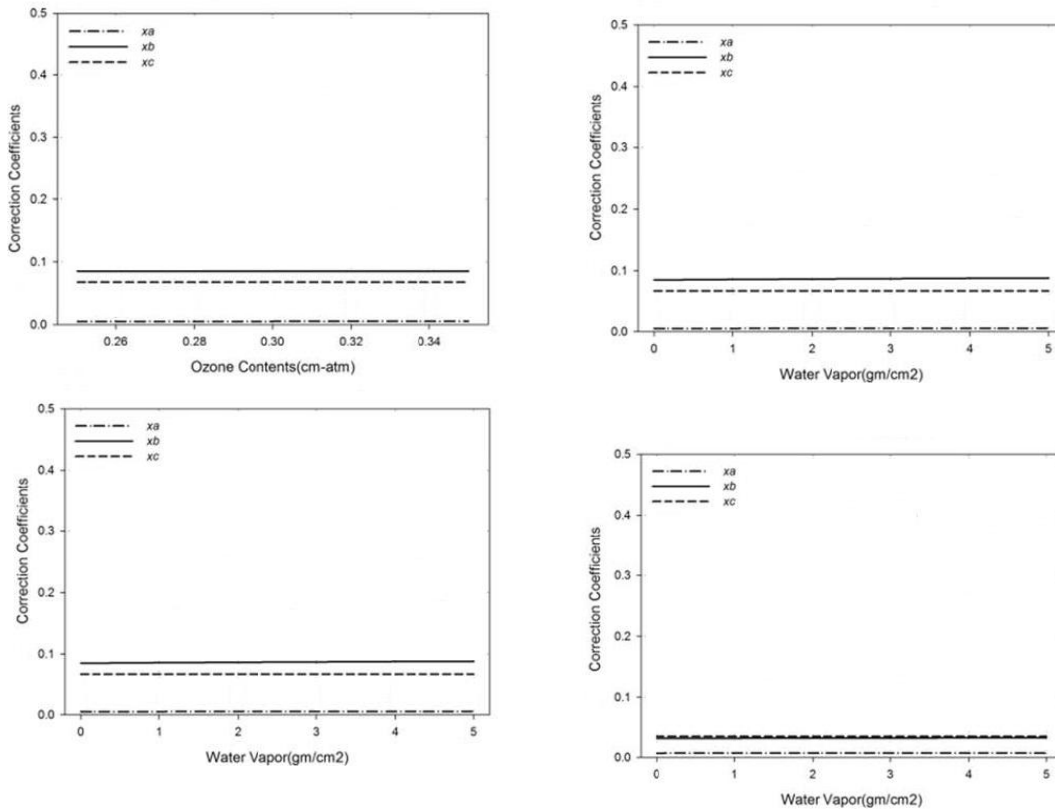


Figure. 4. Sensitivity of correction coefficients to atmospheric parameters (from top to bottom: AOD, ozone, and water vapor) (left: red, right: NIR). The three lines each represent the variation of the correction coefficients (dashdot, solid, and short dash denote xa, xb, and xc, respectively).

The above figure shows the sensitivity of correction coefficients to atmospheric parameters indicating the influence of each input parameter on the correction coefficients in the LUT. The median values of SZA, VZA, solar azimuth angle (SAA), viewing azimuth angle (VAA), AOD, ozone column density, and water vapour were 60°, 60°, 150°, 90°, 0.2, 0.30 cm-atm, and 1 gm cm⁻², respectively.

Table. 2. Result of linear regression analysis of correction coefficients (xb and xc) in the LUT with AOD values.

Co-efficient	R	R ²	Std.error
xb	0.36	0.13	0.183777
xc	0.99	0.88	0.004877

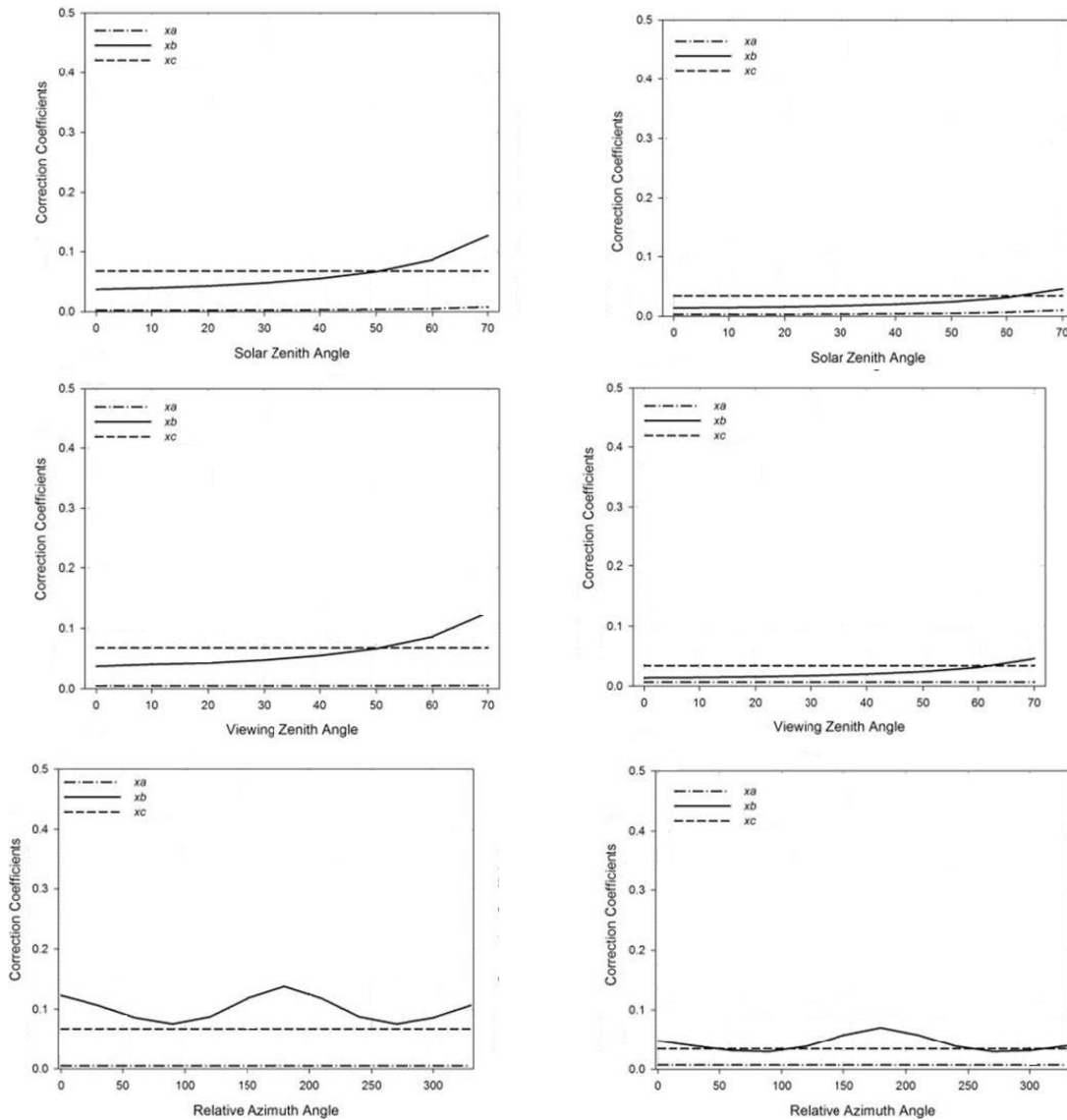


Figure. 5. Sensitivity analysis of correction coefficients with angular data (from top to bottom: SZA, VZA, and RAA) for coarse and fine interval

It is found that the significant variations in the correction coefficients as a function of AOD in the visible bands as shown in the above figure. The effects of ozone and water vapour would be negligible. Thus, regression analyses were carried out for AOD with xb and xc, which had strong sensitivity to the variations in AOD as given in the above table.

A lower root mean-square error (RMSE) was also found for the surface reflectance obtained using the LUT.

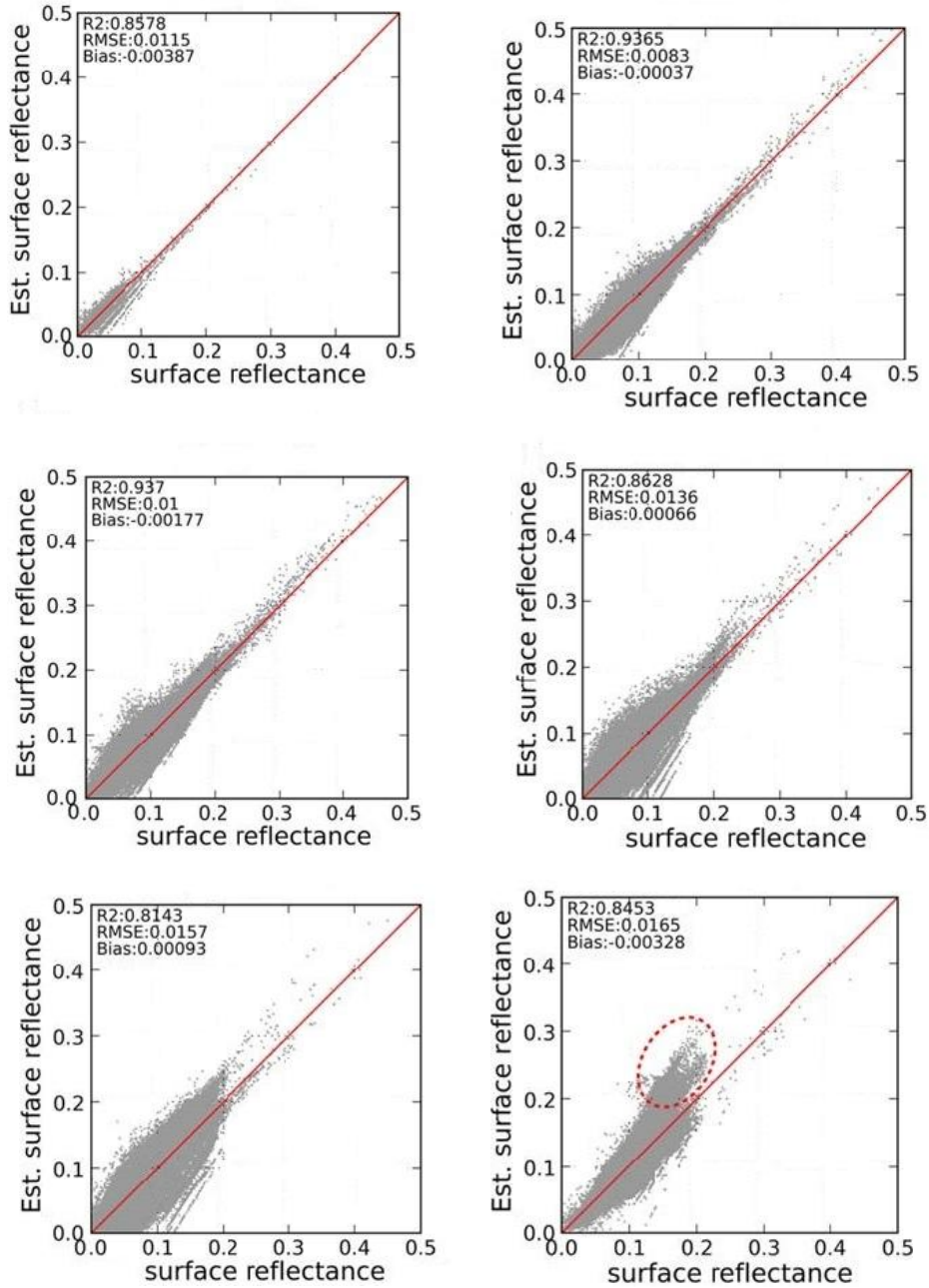


Figure. 6. Scatter plots according to SZA at coarse intervals (Clockwise from top left: 10-20, 20-30, 30-40, 40-50, 50-60 and 60-70)

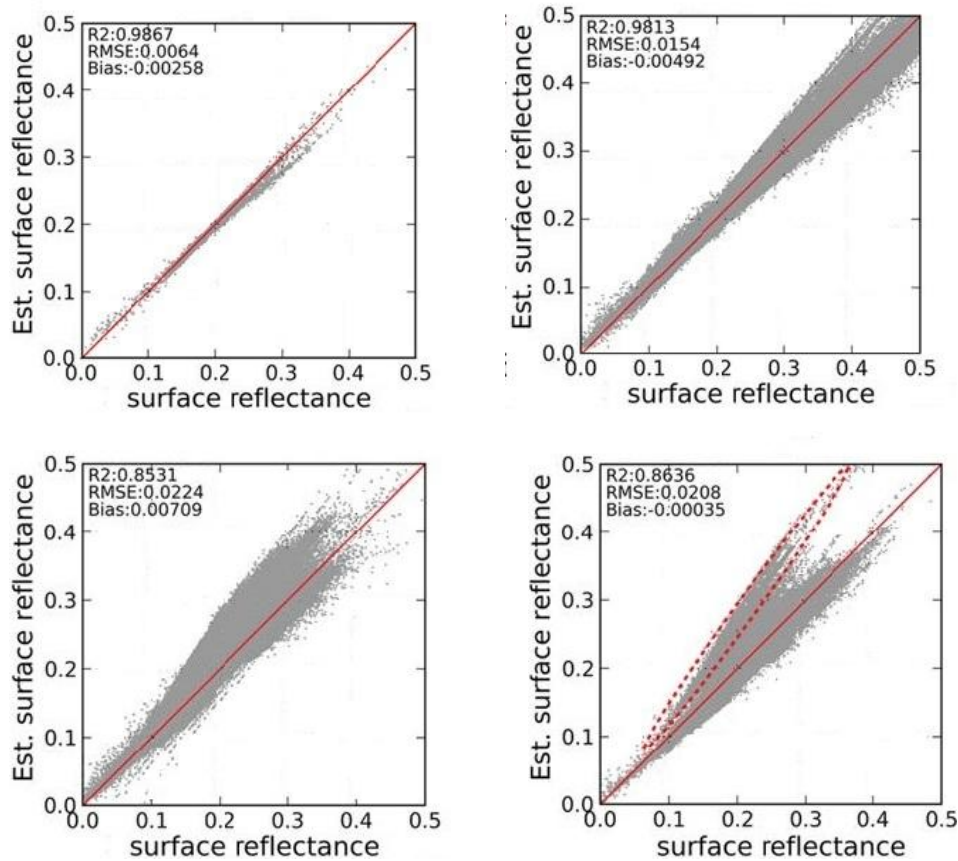


Figure. 7. Scatter plots according to SZA at fine intervals (Clockwise from top left: 40-45, 45-50, 50-55, 55-60, 60-65 and 65-70)

VII. CONCLUSION

Through the test and analysis of this paper, it can be argued that the look-up tables constructed by 6S can satisfy the accuracy required in atmospheric radiation transmission simulation of remote sensing imaging simulation, and calculation efficiency is greatly boost, therefore the construction scheme proposed in this report is feasible. The apparent brightness values of ground targets in sensor pupil obtained by the multi-linear difference value method is with higher precision compared with that obtained by directly calculating with 6S model, and its biggest error is less than 1.2%. Because 6S model operation is time-consuming, so taking the multi-data interpolation algorithm on the basis of meeting the precision requirement is more effective than building a comprehensive look-up tab.

The look-up table generated in this paper is calculated according to the sensor imaging band, it adapts to the simulation of full-colour image, but when it comes to multi-spectrum or hyperspectral remote sensing images simulation, it is necessary to take look-up table with variable wavelength, but this will involve the calculation more time-consuming, and will make the look-up table capacity and storage space becomes very large, so it needs to be further studied.

Limitations

The user interface to 6S have a number of issues and some limitations:

- Every parameter in the input file is specified using a number, even categorical
- Parameters, making the file difficult to read and edit.

- The input file must have exactly the correct format if it is to be read correctly by 6S
- It is only possible to specify one parameter set in the 6S input file, thus running 6S for a range of parameter values requires manually editing the input file between each simulation.
- The format of the 6S output file is easy for humans to read, but hard to extract values from automatically.

VIII. ACKNOWLEDGEMENTS

The Authors thank for the support by the Scientists of Marine and Atmospheric Sciences Department, Indian Institute of Remote Sensing and Staffs of Department of Geography, University of Madras for their support during the study.

REFERENCES

1. C. L. Walthall, J. M. Norman, J. M. Welles, G. Campbell, and B. L. Blad, "Simple equation to approximate the bidirectional reflectance from vegetative canopies and bare soil surface," *Appl. Opt.*, vol. 24, no. 3, pp. 383–387, 1985.
2. Hadjimitsis, D.G and Themistocleous, K. (2009). Aerosol optical thickness determination over Cyprus using satellite remote sensing and ground measurements. *Proceedings of the 29th EARSeL Symposium: Imagin(e/g) Europe -Chania, Crete, Greece, 15-18/6/2009.*
3. Hadjimitsis, D.G, Themistocleous, K., Agapiou, A., Hadjimitsis, M., and Papadavid, G. (2009). Atmospheric correction algorithms intended for air pollution monitoring in Cyprus using satellite remotely sensed data. *Proceedings of the Remote Sensing and Photogrammetric Society-UK, Annual Conference, Leicester, UK, p. 309-314.*
4. Kotchenova, S. Y., Vermote, E. F., Matarrese, R., and Klemm, F. J.: Validation of a vector version of the 6S radiative transfer code for atmospheric correction of satellite data. Part I: Path radiance, *Appl. Optics*, 45, 6762–6774, doi:10.1364/AO.45.006762, 2006
5. Kotchenova, S. Y., and E. F. Vermote, 2007: Validation of a vector version of the 6S radiative transfer code for atmospheric correction of satellite data. Part 2: Homogeneous Lambertian and anisotropic surfaces. *Appl. Optics*, 46, 4455-4464, doi: 10.1364/AO.46.004455.
6. Kotchenova, S., E. Vermote, R. Levy, and A. Lyapustin (2008), Radiative transfer codes for atmospheric correction and aerosol retrieval: intercomparison study, *Appl. Opt.*, 47, 2215–2226.
7. Liang S, Fang H, and Chen M (2001). Atmospheric correction of Landsat ETM+ Land surface imagery-Part 1: Methods. *IEEE Transactions on Geoscience and remote sensing* 39 (11), 2490-2498.
8. Lenoble, J., M. Herman, J. Deuzé, B. Lafrance, R. Santer, and D. Tanré (2007), A successive order of scattering code for solving the vector equation of transfer in the earth's atmosphere with aerosols, *J. Quant. Spectrosc. Radiat. Transfer*, 107, 479–507.
9. Lyapustin, A., John Martonchik, Yujie Wang, Istvan Laszlo, and Sergey Korkin, 2011: Multiangle implementation of atmospheric correction (MAIAC): 1. Radiative transfer basis and look-up tables. *J. Geophys. Res.*, 116, D03210, doi:10.1029/2010JD014985.
10. Min, Q., and M. Duan (2004), A successive order of scattering model for solving vector radiative transfer in the atmosphere, *J. Quant. Spectrosc. Radiat. Transfer*, 87, 243–259.
11. Rahman, H., and G. Dedieu, 1994: SMAC: a simplified method for the atmospheric correction of satellite measurements in the solar spectrum. *Int. J. Remote Sens.*, 15, 123-143.
12. Teillet, P.M. (1992). An algorithm for the radiometric and atmospheric correction of AVHRR data in the solar reflective channels, *Remote sensing of Environment*, 41, 185- 195.
13. Vermote, E.F., Tanré, D, Deuze, J.L., Herman, M., and Morcrette, J.J. (1997) Second Simulation of the Satellite Signal in the Solar Spectrum, 6S: An overview, *IEEE. Transactions in Geoscience Remote Sensing*. GE-35, 675–686.
14. Vermote, E. F., and A. Vermeulen, 1999: Atmospheric Correction Algorithm: SPECTRAL REFLECTANCES (MOD09) version 4.0. Algorithm Technical Background Document (ATBD). http://modis.gsfc.nasa.gov/data/atbd/atbd_mod08.pdf.

15. Vermote, E., D. Tanré, J. Deuzé, M. Herman, J. Morcrette, and S. Y. Kotchenova (2006), *Second simulation of the satellite signal in the solar spectrum (6S), 6S user guide, version 3, part 1*, NASA Goddard Space Flight Center.
16. Zhao, W., Masayuki Tamura, and T. Hidenori, 2000: *Atmospheric and spectral corrections for estimating surface albedo from satellite data using 6S code*. *Remote Sens. Environ.*, 76, 202-212, doi: 10.1016/S0034-4257(00)00204-2.